

# The Transfer Tensor Method: an Analytical Study Case

Marcel Morillas-Rozas <sup>1, \*</sup> Alberto López-García <sup>1</sup> Gonzalo Reina Rivero <sup>1</sup> Jianshu Cao,<sup>2</sup> and Javier Cerrillo <sup>1, †</sup>

<sup>1</sup>*Área de Física Aplicada, Universidad Politécnica de Cartagena member of European University of Technology EUT+, Cartagena E-30202, Spain*

<sup>2</sup>*Department of Chemistry, Massachusetts Institute of Technology, Cambridge, MA 02139, United States of America*

The transfer tensor method is a versatile tool for analyzing and propagating general open quantum systems. It captures in a compact manner all memory effects in a non-Markovian system through a straightforward transformation of a set of dynamical maps. Transfer tensors provide the exact convolutional propagator associated with a given time discretization over the past evolution of an open quantum system. Here we show that, for any finite time discretization, the memory kernel of the Nakajima-Zwanzig equation deviates from the exact transfer tensors, although both converge in the continuous-time limit, as expected. We examine this behaviour in the context of an analytically solvable model: a two level atom resonant with a lossy cavity in the Jaynes-Cummings limit. The atomic dynamics separate into two decoupled degrees of freedom – the coherence and the population inversion. We derive exact expressions for the dynamical map, the transfer tensors and the memory kernel governing the coherence, and we relate them to their counterparts for the population inversion. As a function of the ratio between the cavity loss rate and the atom-cavity coupling strength, we identify regions of enhanced non-Markovianity in which the system can be described as fully Markovian for certain time-step choices.

## I. INTRODUCTION

Transfer tensors (TT) are superoperators that facilitate the propagation and analysis of non-Markovian open quantum systems. They were originally introduced as a way to extract information from short-time trajectories and extrapolate the behaviour of the system to longer times [1]. This is particularly useful in situations where the computational cost increases rapidly with the target simulation time, as is often the case for open quantum systems strongly coupled to an environment and exhibiting non-Markovian behaviour [2, 3]. Transfer tensors can be understood as a transformation of a set of dynamical maps describing the propagation of an open quantum system over a homogeneous time lattice [1, 4].

Since their introduction, TT have found a variety of applications as both a propagation and an analysis tool. Depending on the technique used to calculate the dynamical map, they have been employed, for instance, to extend numerically exact simulations to longer times [5], to account for initially correlated system-environment states [6], to analyze the applicability of discrete-time propagation schemes in open-system dynamics [7], and to characterize non-Markovian noise from reconstructed quantum processes [8]. Their range of applicability has also been studied in detail [9]. Depending on the technique used to calculate the dynamical map, different brands of TT have emerged [10, 11]. In general terms, the transfer tensor method sheds light on the operational meaning of quantum Markovianity [12] and multi-

temporal memory effects can be described with a generalization of the transfer tensor formalism known as the process tensor [13].

These developments are naturally linked to the theory of generalized master equations. In particular, a great deal of effort has been put into the Nakajima-Zwanzig equation (NZE) [14, 15] and practical strategies for building or discretizing its memory kernel [3, 16–19]. TT are closely related to this line of research, however, they are conceptually different objects. They are defined through a discrete family of dynamical maps and, therefore, provide an exact discrete-time representation of the reduced dynamics on a given time lattice [4]. At the zero-timestep limit, they can be connected to the Nakajima-Zwanzig memory kernel, but for finite time steps, the two constructions are not identical. In this sense, transfer tensor method is exact at the selected level of discretization, whereas a direct discretization of the Nakajima-Zwanzig equation generally introduces an additional approximation [4, 18, 19].

In this paper, we analyze their mathematical construction and distinguish it from discretizations of the memory kernel. We resort to a toy model that allows us to derive transfer tensors fully analytically. Their study provides insights into the dynamics such as the existence of Markovian time-discretizations in otherwise fully non-Markovian regimes. This analytical toy model will assist further future analysis on the properties of TTM. This manuscript is structured as follows: In Section II we introduce and compare the transfer tensors and the memory kernel of the Nakajima-Zwanzig equation, and we present the atom-in-a-cavity model used in Section III. Section IV is devoted to the analytical derivation and study of the memory kernels, dynamical maps, and transfer tensors of the system. and V are Finally, we draw

\* marcel.morillas@upct.es

† javier.cerrillo@upct.es

conclusions in Section VI.

## II. THE TRANSFER TENSORS AND THE MEMORY KERNEL

Given a homogeneous discretization of time  $t_k = k\delta t$ , a family of dynamical maps  $\{\mathcal{E}_k\}$  may be defined such that the density matrix of the open quantum system evolves as  $\rho(t_k) = \mathcal{E}_k\rho(0)$ . The transfer tensors are then constructed iteratively from the dynamical maps via

$$\mathcal{T}_k = \mathcal{E}_k - \sum_{j=1}^k \mathcal{T}_j \mathcal{E}_{k-j}, \quad (1)$$

which rewrites the propagation in the exact convolutional form

$$\rho(t_k) = \sum_{j=1}^k \mathcal{T}_j \rho(t_j). \quad (2)$$

An especially insightful object in this hierarchy is the second transfer tensor  $\mathcal{T}_2$ . It quantifies the deviation incurred when attempting to decompose the two-step dynamical map  $\mathcal{E}_2$  into the Markovian composition of two one-step maps, i.e. the error in approximating  $\mathcal{E}_2 \approx \mathcal{E}_1^2$ . In this sense,  $\mathcal{T}_2$  provides a direct measure of the memory effects generated between the first and second time steps. This connects naturally to established notions of quantum non-Markovianity, where memory effects are associated either with the breakdown of CP-divisibility [20] or with the revival of information flow as quantified, for instance, by trace-distance backflow [21]. The magnitude of  $\mathcal{T}_2$  may therefore be interpreted as a discrete-time analogue of these criteria, capturing the first departure from Markovian composition at finite resolution.

It is instructive to relate the transfer-tensor construction to its underlying enlarged-space formulation. A dynamical map can always be expressed as the projection of a multiplicative temporal evolution of a larger space  $\mathcal{U}$  with projector  $\mathcal{P}$ . For a time homogeneous evolution one has  $\mathcal{U}(k\delta t) = \mathcal{U}^k$ , and therefore  $\mathcal{E}_k = \mathcal{P}\mathcal{U}^k\mathcal{P}$ . Within this representation, the  $k$ -th transfer tensor takes the compact form

$$\mathcal{T}_k = \mathcal{P}\mathcal{U}\mathcal{Q}(\mathcal{Q}\mathcal{U}\mathcal{Q})^{k-2}\mathcal{Q}\mathcal{U}\mathcal{P}, \quad (3)$$

where  $\mathcal{Q} = 1 - \mathcal{P}$  denotes the complementary projector. The memory kernel (MK) of the Nakajima-Zwanzig formalism is defined differently. Starting from the first order differential equation satisfied by  $\mathcal{U}$

$$\frac{d}{dt}\mathcal{U} = \mathcal{L}\mathcal{U}, \quad (4)$$

the action of  $\mathcal{P}$  yields a closed integrodifferential equation for the dynamical map

$$\frac{d}{dt}\mathcal{E}(t) = \mathcal{P}\mathcal{L}\mathcal{P}\mathcal{E}(t) + \int_0^t \mathcal{K}(t-s)\mathcal{E}(s)ds, \quad (5)$$

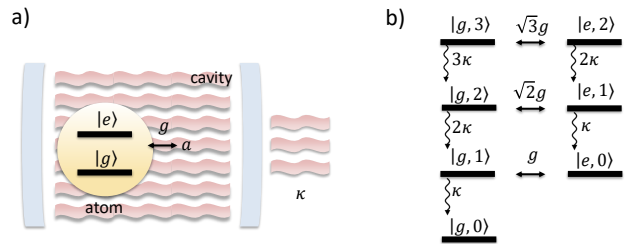


FIG. 1. a) Diagram of the considered atom-cavity model. The atom is represented by two levels  $|e\rangle$  and  $|g\rangle$ . The cavity loses photons at a rate  $\kappa$ . Cavity and atom are coupled by a Jaynes-Cummings term of strength  $g$ . b) Level diagram representing the lowest states of the full Hilbert space, the strength of the couplings among themselves and the decay rates.

with memory kernel

$$\mathcal{K}(t) = \mathcal{P}\mathcal{L}\mathcal{Q} \exp(\mathcal{Q}\mathcal{L}\mathcal{Q}t) \mathcal{Q}\mathcal{L}\mathcal{P}. \quad (6)$$

Although the transfer tensor and the memory kernel differ significantly at any finite time discretization, both converge in the continuous-time limit

$$\lim_{k \rightarrow \infty} \frac{\mathcal{T}_k(t/k)}{t^2/k^2} = \mathcal{K}(t), \quad (7)$$

as shown in Appendix A. Hence, they cannot coincide at finite  $k$ . Since the transfer tensors arise from an exact transformation of the exact dynamical maps, any finite-step representation of the memory kernel is necessarily subject to discretization error.

## III. THE JAYNES-CUMMINGS MODEL

In order to investigate the differences, let us consider an analytically solvable model consisting of a two-level atom of states  $|e\rangle$  and  $|g\rangle$  coupled to a single mode of a lossy cavity in the Jaynes Cummings limit (see Fig.1a). In a suitable rotating frame, the Hamiltonian reads

$$\hat{H} = g\hat{\sigma}^+\hat{a} + \text{H.c.}, \quad (8)$$

where  $\hat{\sigma}^+ = |\uparrow\rangle\langle\downarrow|$  and  $\hat{a}, \hat{a}^\dagger$  are the bosonic ladder operators of the cavity mode. The master equation that describes the Markovian temporal evolution of the system reads

$$\frac{d}{dt}\hat{\mu} = [\hat{H}, \hat{\mu}] + \kappa \left( \hat{a}\hat{\mu}\hat{a}^\dagger - \frac{1}{2}\hat{a}^\dagger\hat{a}\hat{\mu} - \frac{1}{2}\hat{\mu}\hat{a}\hat{a}^\dagger \right). \quad (9)$$

For a cavity initialized in its stationary state  $|0\rangle$ , just three states contribute to the dynamics:  $|e\rangle = |\uparrow, 0\rangle$ ,  $|i\rangle = |\downarrow, 1\rangle$  and  $|g\rangle = |\downarrow, 0\rangle$  (see Fig.1b). We may then define the populations  $p_k = \langle k|\hat{\mu}|k\rangle$  and the coherences  $c_{jk} = \langle j|\hat{\mu}|k\rangle = c_{kj}^*$ . The dynamics of the system decouples into two subspaces: on the one hand, subspace  $A$  involving  $\{p_e, p_i, p_g, c_{ei}\}$  and, on the other hand, subspace

$B$  containing  $\{c_{eg}, c_{ig}\}$ . Based on this decomposition, we may express the Liouvillian governing the dynamics as  $\mathcal{L} = \mathcal{L}_A \oplus \mathcal{L}_B$ .

We now focus on the two level atom as our open quantum system of interest. This offers a minimal testing ground to analyze the effect that the strength of the coupling to the environment (represented by  $g$ ) and the timescale of the bath (proportional to  $\kappa^{-1}$ ) has on the Markovianity of the atom. The reduced density matrix of the system  $\hat{\rho}$  contains elements  $p_{\uparrow} = p_e$ ,  $p_{\downarrow} = p_g + p_i$  and  $c = c_{eg}$ . The  $A$ - $B$  decomposition proves especially useful, as it enables us to derive the dynamical maps, transfer tensors, and memory kernels for both the population inversion  $\delta p = p_{\uparrow} - p_{\downarrow}$  and the coherence  $c$  independently, and to express them as scalars rather than tensors.

#### IV. COHERENCE SUBSPACE

For the smaller subspace  $B$  the dynamical equations derived from Eq. (9) for the coherences  $\{c_{eg}, c_{ig}\}$  read

$$\dot{c}_{eg} = -igc_{ig}, \quad (10)$$

$$\dot{c}_{ig} = -igc_{eg} - \frac{\kappa}{2}c_{ig}, \quad (11)$$

which may be expressed in matrix form  $\dot{\mathbf{c}} = \mathcal{L}_B \mathbf{c}$  with

$$\mathbf{c} = \begin{pmatrix} c_{eg} \\ c_{ig} \end{pmatrix}; \quad \mathcal{L}_B = \begin{pmatrix} 0 & -ig \\ -ig & -\kappa/2 \end{pmatrix}. \quad (12)$$

The projection superoperators in this subspace become the matrices  $\mathcal{P}_B = 1 \oplus 0$  and  $\mathcal{Q}_B = 0 \oplus 1$  which yield  $\mathcal{Q}_B \mathcal{L}_B \mathcal{Q}_B = -\kappa \mathcal{Q}_B / 2$  and  $\mathcal{P}_B \mathcal{L}_B \mathcal{Q}_B \mathcal{L}_B \mathcal{P}_B = -g^2 \mathcal{P}_B$ , both elements required to calculate the memory kernel component for the coherence  $c$

$$\mathcal{K}_c(t) = -g^2 e^{-\kappa t/2}. \quad (13)$$

To obtain the dynamical map and transfer-tensor components, we perform the eigendecomposition of  $\mathcal{L}_B$ . The eigenvalues are  $\kappa_{\pm} = -\kappa/4 \pm \sqrt{(\kappa/4)^2 - g^2}$  and the projectors associated to their respective eigenvectors

$$\mathcal{P}_{\pm} = \frac{1}{\kappa_{\mp} - \kappa_{\pm}} \begin{pmatrix} \kappa_{\mp} & ig \\ ig & -\kappa_{\pm} \end{pmatrix}. \quad (14)$$

This provides  $\mathcal{U}_B = \mathcal{P}_+ e^{\kappa_+ t} + \mathcal{P}_- e^{\kappa_- t}$ , which contains a component of the dynamical map

$$\mathcal{E}_c(t) = \frac{\kappa_+ e^{\kappa_- t} - \kappa_- e^{\kappa_+ t}}{\kappa_+ - \kappa_-}. \quad (15)$$

Depending on the quotient  $\kappa/4g$ , overdamped, critically damped and underdamped regimes may be distinguished in the dynamics of the coherence  $c(t) = \mathcal{E}_c(t)c(0)$ , as shown in Fig. 2.

We may now construct the second transfer tensor associated with the coherence,

$$\mathcal{T}_{2,c} \mathcal{P}_B = \mathcal{P}_B \mathcal{U}_B \mathcal{Q}_B \mathcal{U}_B \mathcal{P}_B = - \left( g \frac{e^{\kappa_- t} - e^{\kappa_+ t}}{\kappa_+ - \kappa_-} \right)^2 \mathcal{P}_B. \quad (16)$$

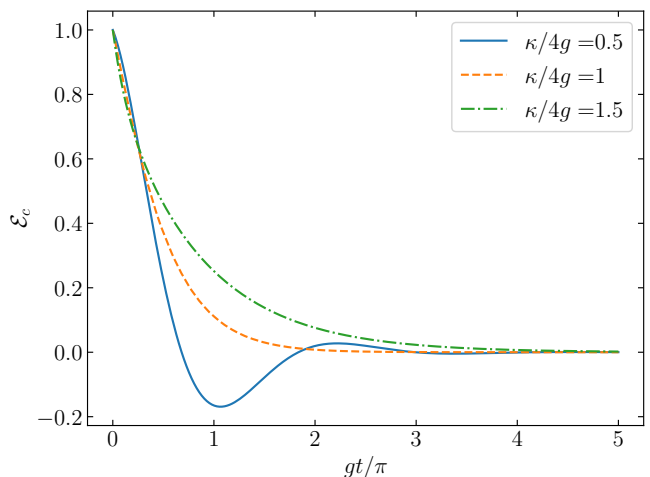


FIG. 2. Temporal evolution of the coherence dynamical map  $\mathcal{E}_c$  for different values of  $\kappa/4g$ , illustrating the underdamped (solid line), overdamped (dot-dashed line) and critically damped (dashed line) regimes.

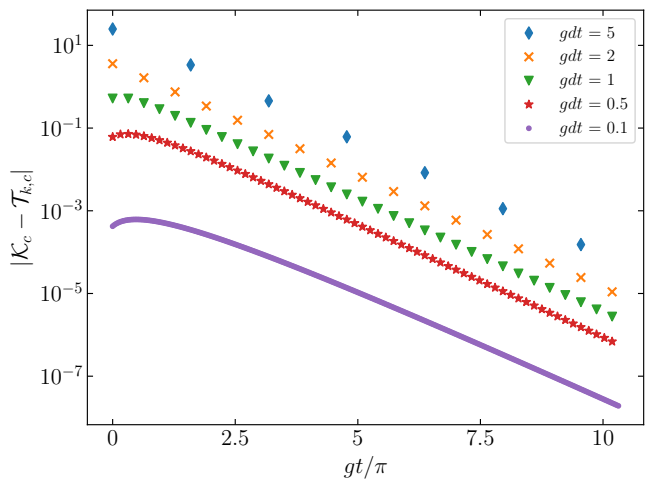


FIG. 3. Absolute value of the difference between the memory kernel  $\mathcal{K}_c$  and the transfer tensor  $\mathcal{T}_{k,c}$  for different timestep values and  $\kappa/4g = 0.2$ , showing that  $\mathcal{T}_{k,c}$  converges to  $\mathcal{K}_c$  as the timestep is reduced.

Together with the scalar  $\mathcal{Q}_B \mathcal{U}_B \mathcal{Q}_B$  this expression allows us to obtain all higher-order transfer-tensor components for the coherence sector:

$$\mathcal{T}_{k,c}(t) = \mathcal{T}_{2,c} \left( \frac{\kappa_+ e^{\kappa_+ t} - \kappa_- e^{\kappa_- t}}{\kappa_+ - \kappa_-} \right)^{k-2} \quad (17)$$

One can verify that this result satisfies Eq. (7), as expected. This behavior is illustrated in Fig. 3: as the time discretization becomes finer, the difference between the memory kernel  $\mathcal{K}_c(t)$  and the transfer tensor  $\mathcal{T}_{k,c}$  correspondingly decreases.

Interestingly, while the memory kernel always decays monotonically, the transfer tensors retain explicit infor-

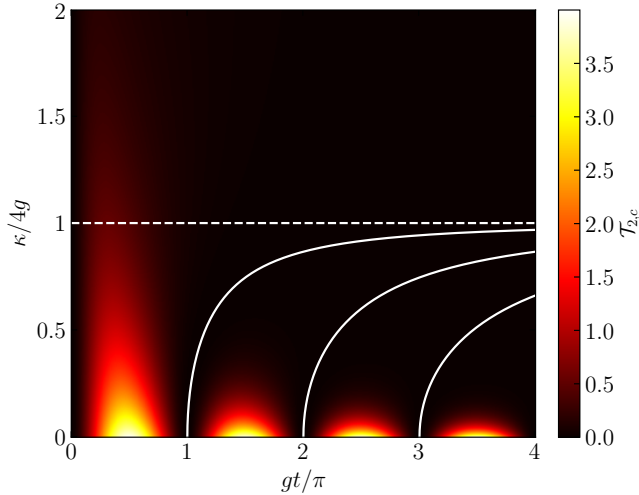


FIG. 4.  $\mathcal{T}_{2,c}$  as a function of  $gt$  and  $\kappa/4g$ . The dashed line corresponds to the frontier between the underdamped and the overdamped regimes. The solid lines show the zeros of  $\mathcal{T}_{2,c}$  where the evolution of the system is guaranteed to be fully Markovian.

mation about the dynamical regime of the system. Figure 4 illustrates this by showing  $\mathcal{T}_{2,c}(t)$  for different values of the ratio  $\kappa/4g$ . In the underdamped regime,  $\mathcal{T}_{2,c}(t)$  can be written as

$$\mathcal{T}_{2,c}(t) = 4g^2 t^2 e^{-\frac{\kappa t}{2}} \text{sinc}^2 \left[ gt \sqrt{1 - \left( \frac{\kappa}{4g} \right)^2} \right], \quad (18)$$

which vanishes whenever the argument of the sinc function is proportional to  $\pi$ . Since all coherence-sector transfer tensors scale with  $\mathcal{T}_{2,c}$ , as seen in Eq. (17), these zeros mark the timesteps at which concatenation of the dynamical map introduces no error. In other words, such points correspond to Markovian discretizations. Thus, full Markovianity arises precisely when the timestep matches the oscillation period of the coherences in the underdamped regime, as shown in Fig. 5, where the zeros of  $\mathcal{T}_{2,c}(t)$  align with the periodicity of the coherence dynamics.

## V. POPULATION SUBSPACE

Subspace  $A$  contains the three populations  $p_e, p_i, p_g$  together with the imaginary part of coherence  $c_{ei}$ . Their evolution is governed by

$$\dot{p}_e = -2gc_{ei}^i, \quad (19)$$

$$\dot{p}_i = -\kappa p_i + 2gc_{ei}^i, \quad (20)$$

$$\dot{p}_g = \kappa p_i, \quad (21)$$

$$\dot{c}_{ei}^i = g(p_e - p_i) - \frac{\kappa}{2} c_{ei}^i, \quad (22)$$

where  $c_{ei}^i \equiv \text{Im}(c_{ei})$ . It is convenient to introduce the relevant variable  $\delta p = p_\uparrow - p_\downarrow$  and the irrelevant variables

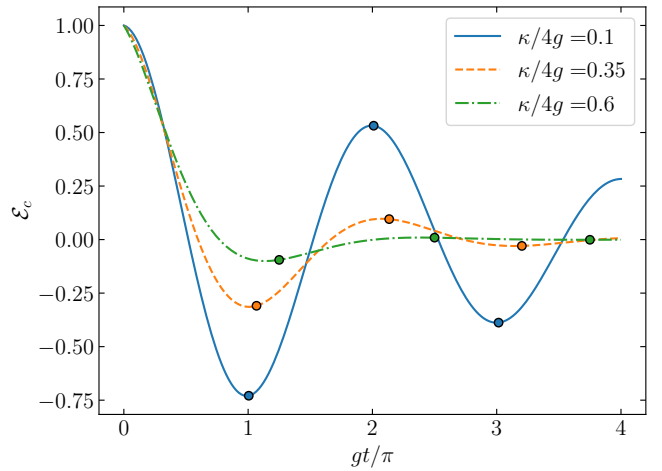


FIG. 5. Temporal evolution of the coherence dynamical map  $\mathcal{E}_c$  in the underdamped regime. The dots on each line correspond to the three first zeros of  $\mathcal{T}_{2,c}(t)$ , where the evolution is fully Markovian for that given timestep.

$c_{ei}^i$  and  $\delta p' = p_i - p_g$ . In terms of these, the equations become  $\dot{\mathbf{p}} = \mathcal{L}_A \mathbf{p}$  with

$$\mathbf{p} = \begin{pmatrix} \delta p \\ c_{ei}^i \\ \delta p' \\ 1 \end{pmatrix}; \quad \mathcal{L}_A = \begin{pmatrix} 0 & -4g & 0 & 0 \\ 3g/4 & -\kappa/2 & -g/2 & g/4 \\ \kappa/2 & 2g & -\kappa & -\kappa/2 \\ 0 & 0 & 0 & 0 \end{pmatrix}.$$

The projection superoperators in this subspace are  $\mathcal{P}_A = 1 \oplus 0_{3 \times 3}$  and  $\mathcal{Q}_A = 0 \oplus 1_{3 \times 3}$ .

To obtain the memory kernel, it is necessary to exponentiate the matrix  $\mathcal{Q}_A \mathcal{L}_A \mathcal{Q}_A$ . Following the same procedure as in Sec. IV we derive the corresponding expressions (see Appendix. C) and find that it may be written in terms of dynamical objects of the coherence subspace:

$$\mathcal{K}_p(t) = \mathcal{K}_c(t) \left[ \mathcal{E}_c(t) + 2 \frac{\mathcal{T}_{3,c}}{\mathcal{T}_{2,c}} \right]. \quad (23)$$

Comparing the population component of the memory kernel with its coherence counterpart shows that the population sector acquires a biexponential form, with regimes of underdamping and critical damping.

For the dynamical map, the matrix  $\mathcal{L}_A$  can be analytically exponentiated, leading to a compact expression that connects the population dynamics to quantities from the coherence subspace:

$$\mathcal{E}_p(t) = \mathcal{E}_c^2(t) + \frac{1}{2} \mathcal{T}_{2,c}. \quad (24)$$

This shows that the population dynamics follows the coherence dynamics except when non-Markovian effects - encoded in the second transfer tensor of the coherence sector - become relevant. Using Eq. (24), the second transfer tensor of the populations is obtained as

$$\mathcal{T}_{2,p} = \frac{3}{2} \mathcal{T}_{2,c} \mathcal{E}_p + \mathcal{T}_{3,c} \mathcal{E}_c + \frac{1}{2} \mathcal{T}_{4,c}, \quad (25)$$

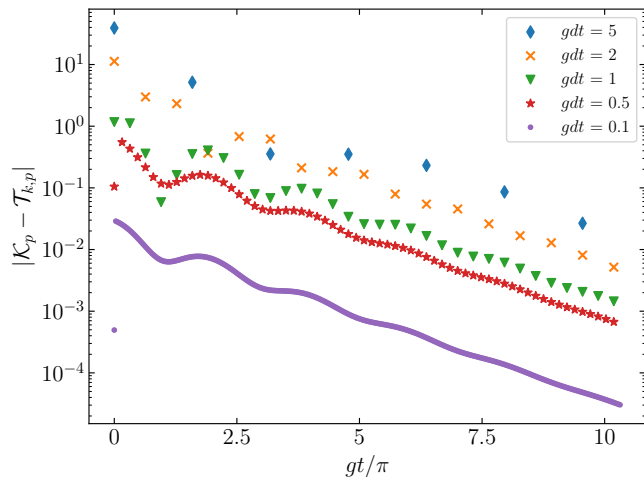


FIG. 6. Absolute value of the difference between the memory kernel  $\mathcal{K}_p$  and the transfer tensor  $\mathcal{T}_{k,p}$  for different timestep values and  $\kappa/4g = 0.2$ , showing that  $\mathcal{T}_{k,c}$  converges to  $\mathcal{K}_c$  as the timestep is reduced.

as derived in Appendix. E. Importantly,  $\mathcal{T}_{2,p}$  remains proportional to  $\mathcal{T}_{2,c}$  and therefore inherits the same regions

of Markovian timesteps.

Finally, the remaining transfer tensors can be obtained analytically by combining Eq. (24) with the expressions derived for the coherence sector. As in the case of the coherences, any finite discretization of the population memory kernel  $\mathcal{K}_p$  deviates from the exact transfer tensor  $\mathcal{T}_{k,p}$ . Nevertheless, this deviation decreases as the timestep is reduced, in accordance with Eq. (7) and as illustrated in Fig. 6.

## VI. CONCLUSION

We have demonstrated that the transfer tensors and the Nakajima-Zwanzig memory kernel are fundamentally distinct mathematical objects, converging only in the limit of an infinitesimal time-step. By applying this framework to the analytically solvable Jaynes-Cummings model, we have identified three distinct dynamical regimes. Notably, our results indicate that Markovian behavior is restricted to the underdamped regime. Finally, we have identified that the dynamics of the populations and the coherences are related by the second transfer tensor.

- 
- [1] J. Cerrillo and J. Cao, Non-markovian dynamical maps: Numerical processing of open quantum trajectories, *Phys. Rev. Lett.* **112**, 110401 (2014).
  - [2] I. de Vega and D. Alonso, Dynamics of non-markovian open quantum systems, *Rev. Mod. Phys.* **89**, 015001 (2017).
  - [3] D. S. Briand and E. Geva, Generalized quantum master equation: A tutorial review and recent developments, *Chinese J. Chem. Phys.* **34**, 845 (2021).
  - [4] F. A. Pollock and K. Modi, Tomographically reconstructed master equations for any open quantum dynamics, *Quantum* **2**, 76 (2018).
  - [5] R. Rosenbach, J. Cerrillo, S. F. Huelga, J. Cao, and M. B. Plenio, Efficient simulation of non-markovian system-environment interaction, *New J. Phys.* **18**, 023035 (2016).
  - [6] M. Buser, J. Cerrillo, G. Schaller, and J. Cao, Initial system-environment correlations via the transfer-tensor method, *Phys. Rev. A* **96**, 062122 (2017).
  - [7] M. Cygorek, A. M. Barth, F. Ungar, A. Vagov, and V. M. Axt, Nonlinear cavity feeding and unconventional photon statistics in solid-state cavity qed revealed by many-level real-time path-integral calculations, *Physical Review B* **96**, 201201 (2017).
  - [8] Y.-Q. Chen, K.-L. Ma, Y.-C. Zheng, J. Allcock, S. Zhang, and C.-Y. Hsieh, Non-markovian noise characterization with the transfer tensor method, *Phys. Rev. Applied* **13**, 034045 (2020).
  - [9] A. Gelzinis, E. Rybakovas, and L. Valkunas, Applicability of transfer tensor method for open quantum system dynamics, *J. Chem. Phys.* **147**, 234108 (2017).
  - [10] N. Makri, Small matrix path integral for system-bath dynamics, *J. Chem. Theory Comput.* **16**, 4038 (2020).
  - [11] G. Wang and Z. Cai, Tree-based implementation of the small matrix path integral for system-bath dynamics, *Commun. Comput. Phys.* **36**, 389 (2024).
  - [12] F. A. Pollock, S. Milz, D. Egloff, M. Paternostro, and K. Modi, Operational markov condition for quantum processes, *Phys. Rev. Lett.* **120**, 040405 (2018).
  - [13] F. A. Pollock, C. Rodríguez-Rosario, T. Frauenheim, M. Paternostro, and K. Modi, Non-markovian quantum processes: Complete framework and efficient characterization, *Phys. Rev. A* **97**, 012127 (2018).
  - [14] S. Nakajima, On quantum theory of transport phenomena: Steady diffusion, *Progress of Theoretical Physics* **20**, 948 (1958).
  - [15] R. Zwanzig, Ensemble method in the theory of irreversibility, *The Journal of Chemical Physics* **33**, 1338 (1960).
  - [16] Q. Shi and E. Geva, A new approach to calculating the memory kernel of the generalized quantum master equation for an arbitrary system-bath coupling, *J. Chem. Phys.* **119**, 12063 (2003).
  - [17] A. Kelly, A. Montoya-Castillo, L. Wang, and T. E. Markland, Generalized quantum master equations in and out of equilibrium: When can one win?, *J. Chem. Phys.* **144**, 184105 (2016).
  - [18] N. Makri, Discrete generalized quantum master equations, *J. Chem. Theory Comput.* **21**, 5037 (2025).
  - [19] R. Peng, L. P. Lindoy, and J. Lee, On the discretization error of the discrete generalized quantum master equation, *J. Chem. Phys.* **163**, 134101 (2025).
  - [20] Á. Rivas, S. F. Huelga, and M. B. Plenio, Entanglement and non-markovianity of quantum evolutions, *Physical Review Letters* **105**, 050403 (2010).

- [21] H.-P. Breuer, E.-M. Laine, and J. Piilo, Measure for the degree of non-markovian behavior of quantum processes, *Physical Review Letters* **103**, 210401 (2009).

### Appendix A: Limit TTM to Memory Kernel

The calculation of the limit of the TTM to the memory kernel only for small timestep is as follows

$$\lim_{k \rightarrow \infty} \frac{\mathcal{T}_k(t/k)}{t^2/k^2} = \lim_{k \rightarrow \infty} \mathcal{P} \left( 1 + \frac{t}{k} \mathcal{L} \right) \left[ \mathcal{Q} \left( 1 + \frac{t}{k} \mathcal{L} \right) \right]^{k-1} \mathcal{P} \quad (\text{A1})$$

$$= \mathcal{P} \mathcal{L} \mathcal{Q} \lim_{k \rightarrow \infty} \left( 1 + \frac{t}{k} \mathcal{Q} \mathcal{L} \mathcal{Q} \right)^{k-2} \mathcal{Q} \mathcal{L} \mathcal{P} \quad (\text{A2})$$

The remaining limit is the definition of the exponential

$$\lim_{k \rightarrow \infty} \left( 1 + A \frac{t}{k} \mathcal{Q} \mathcal{L} \mathcal{Q} \right)^{k-2} = e^{At}. \quad (\text{A3})$$

up to a correction of order  $k^{-2}$ .

### Appendix B: Eigensystem of Subspace B

Simplified expression for the coherence, where the associated memory kernel appears

$$\dot{c}(t) = -g^2 \int_0^t e^{-\kappa(t-s)/2} c(s) ds. \quad (\text{B1})$$

For the transfer tensors, the full exponential of  $\mathcal{L}_B$  is needed. In order to compute it, we will use its spectral decomposition. The eigenvalues of

$$\mathcal{L}_B = \begin{pmatrix} 0 & -ig \\ -ig & -\kappa/2 \end{pmatrix} \quad (\text{B2})$$

are the solutions to the characteristic polynomial

$$\lambda^2 + \kappa\lambda/2 + g^2 = 0, \quad (\text{B3})$$

which read

$$\kappa_{\pm} = -\frac{\kappa}{4} \pm \frac{\sqrt{\kappa^2/4 - 4g^2}}{2}. \quad (\text{B4})$$

The corresponding right eigenvectors read

$$\mathbf{v}_{\pm} = \begin{pmatrix} -ig \\ \kappa_{\pm} \end{pmatrix}, \quad (\text{B5})$$

and the left eigenvectors are simply  $\mathbf{w}_{\pm} = \mathbf{v}_{\pm}^T$  due to the fact that  $\mathcal{L}_B = \mathcal{L}_B^T$ . The associated projectors are obtained as

$$\mathcal{P}_{\pm} = \frac{\mathbf{v}_{\pm} \mathbf{w}_{\pm}}{\mathbf{w}_{\pm} \mathbf{v}_{\pm}} = \frac{1}{\kappa_{\pm}^2 - g^2} \begin{pmatrix} -g^2 & -ig\kappa_{\pm} \\ -ig\kappa_{\pm} & \kappa_{\pm}^2 \end{pmatrix} \quad (\text{B6})$$

which simplify to

$$\mathcal{P}_{\pm} = \frac{1}{\kappa_{\mp} - \kappa_{\pm}} \begin{pmatrix} \kappa_{\mp} & ig \\ ig & -\kappa_{\pm} \end{pmatrix}. \quad (\text{B7})$$

as a consequence of the invariance of the determinant  $\kappa_+ \kappa_- = g^2$ .

### Appendix C: Populations Memory Kernel

To compute the populations memory kernel, we need to compute the exponential matrix  $\exp(\mathcal{Q}_A \mathcal{L}_A \mathcal{Q}_A t)$ , which will be done by using the eigendecomposition of that matrix. The eigenvalues of

$$\mathcal{Q}_A \mathcal{L}_A \mathcal{Q}_A = 0 \oplus \begin{pmatrix} -\kappa/2 & -g/2 & g/4 \\ 2g & -\kappa & -\kappa/2 \\ 0 & 0 & 0 \end{pmatrix}. \quad (\text{C1})$$

The first block has eigenvalue 0, and the eigenvalues of the  $3 \times 3$  block are the solution to the polynomial

$$-\lambda \left[ \left( \frac{\kappa}{2} + \lambda \right) (\kappa + \lambda) + g^2 \right] = 0, \quad (\text{C2})$$

which read  $\lambda_0 = 0$  and

$$\lambda_{\pm} = -\frac{3\kappa}{4} \pm \frac{\sqrt{\kappa^2/4 - 4g^2}}{2} = -\frac{\kappa}{2} + \kappa_{\pm} \quad (\text{C3})$$

and produce the right eigenvectors

$$\mathbf{v}_{\pm} = \begin{pmatrix} \kappa_{\mp} \\ -2g \\ 0 \end{pmatrix}, \quad \mathbf{v}_0 = \begin{pmatrix} \kappa g \\ g^2 - \kappa^2/2 \\ 2g^2 + \kappa^2 \end{pmatrix}, \quad (\text{C4})$$

and left eigenvectors

$$\mathbf{w}_{\pm}^T = \begin{pmatrix} \kappa_{\mp} \\ g/2 \\ \frac{g}{2} \frac{\kappa_{\mp} - \kappa}{2\kappa_{\pm} - \kappa} \end{pmatrix}, \quad \mathbf{w}_0^T = \begin{pmatrix} 0 \\ 0 \\ 1 \end{pmatrix}, \quad (\text{C5})$$

which are the solution to  $\mathcal{L}_A \mathbf{w}_{\lambda}^T = \lambda \mathbf{w}_{\lambda}^T$ . The associated projectors for the  $3 \times 3$  block are

$$\mathcal{P}_0 = \frac{\mathbf{v}_0 \mathbf{w}_0^T}{\mathbf{w}_0 \mathbf{v}_0} = \frac{1}{\kappa^2 + 2g^2} \begin{pmatrix} 0 & 0 & \kappa g \\ 0 & 0 & g^2 - \kappa^2/2 \\ 0 & 0 & 2g^2 + \kappa^2 \end{pmatrix}, \quad (\text{C6})$$

and

$$\mathcal{P}_{\pm} = \frac{\mathbf{v}_{\pm} \mathbf{w}_{\pm}^T}{\mathbf{w}_{\pm} \mathbf{v}_{\pm}} = \frac{1}{\kappa_{\mp} - \kappa_{\pm}} \begin{pmatrix} \kappa_{\mp} & g/2 & \frac{g}{2} \frac{\kappa_{\mp} - \kappa}{2\kappa_{\pm} - \kappa} \\ -2g & -\kappa_{\pm} & -\kappa_{\pm} \frac{\kappa_{\mp} - \kappa}{2\kappa_{\pm} - \kappa} \\ 0 & 0 & 0 \end{pmatrix}, \quad (\text{C7})$$

$$\mathcal{P}_{\pm} = \frac{-\kappa_{\pm}}{(\kappa_{+} - \kappa_{-})^2} \begin{pmatrix} \kappa_{\mp}/2 - \kappa_{\pm} & -4g & -\kappa_{\mp} & (\kappa_{\mp} + \kappa)/2 \\ g(1/2 - \kappa_{\mp}/4\kappa_{\pm}) & 2\kappa_{\mp} & -g\kappa_{\mp}/2\kappa_{\pm} & g(1/2 + \kappa_{\mp}/4\kappa_{\pm}) \\ \kappa/4(1 - \kappa_{\mp}/\kappa_{\pm}) - 3\kappa_{\mp}/4 & -2g(1 + 2\kappa_{\mp}/\kappa_{\pm}) & \kappa\kappa_{\mp}/2\kappa_{\pm} - 2\kappa_{\mp} & (2g^2 + \kappa^2)/8\kappa_{\pm} \\ 0 & 0 & 0 & 0 \end{pmatrix}. \quad (\text{D5})$$

### Appendix E: Derivation of $\mathcal{T}_{2,p}$

Starting from the general expression for the  $k$ -th transfer tensor  $\mathcal{T}_k$  from Eq. (3), it is immediate to see that the

from which the memory kernel can be extracted as

$$\mathcal{K}_p(t) = \mathcal{K}_c(t) \frac{(\kappa_{+} - 2\kappa_{-})e^{\kappa_{-}t} - (\kappa_{-} - 2\kappa_{+})e^{\kappa_{+}t}}{\kappa_{+} - \kappa_{-}}. \quad (\text{C8})$$

### Appendix D: Eigensystem of Subspace A

We consider the matrix  $\mathcal{L}_A$

$$\mathcal{L}_A = \begin{pmatrix} 0 & -4g & 0 & 0 \\ 3g/4 & -\kappa/2 & -g/2 & g/4 \\ \kappa/2 & 2g & -\kappa & -\kappa/2 \\ 0 & 0 & 0 & 0 \end{pmatrix}. \quad (\text{D1})$$

Its characteristic polynomial

$$\frac{1}{2}\gamma(2\lambda + \kappa)(4g^2 + \gamma[\gamma + \kappa]) = 0, \quad (\text{D2})$$

yields eigenvalues  $\gamma_0 = 0$ ,  $\gamma_1 = -\kappa/2$  and  $\gamma_{\pm} = 2\kappa_{\pm}$  and the associated projectors are

$$\mathcal{P}_0 = \begin{pmatrix} 0 & 0 & 0 & -1 \\ 0 & 0 & 0 & 0 \\ 0 & 0 & 0 & -1 \\ 0 & 0 & 0 & 1 \end{pmatrix}, \quad (\text{D3})$$

$$\mathcal{P}_1 = \frac{-g}{(\kappa_{+} - \kappa_{-})^2} \begin{pmatrix} g & -2\kappa & 2g & 3g \\ \kappa/8 & -\kappa^2/4g & \kappa/4 & 3\kappa/8 \\ 3g/2 & -3\kappa & 3g & 9g/2 \\ 0 & 0 & 0 & 0 \end{pmatrix}, \quad (\text{D4})$$

$\mathcal{T}_2$  is obtained as

$$\mathcal{T}_{2,p} = \mathcal{P}_A \mathcal{U}_A \mathcal{Q}_A \mathcal{U}_A \mathcal{P}_A. \quad (\text{E1})$$

Using the fact that  $\mathcal{P}_A, \mathcal{Q}_A$  are projectors, we can express  $\mathcal{Q}_A = 1 - \mathcal{P}_A$  and rewrite the  $\mathcal{T}_{2,p}$  as

$$\mathcal{T}_{2,p} = \mathcal{P}_A \mathcal{U}_A \mathcal{U}_A \mathcal{P}_A - \mathcal{P}_A \mathcal{U}_A \mathcal{P}_A \mathcal{U}_A \mathcal{P}_A. \quad (\text{E2})$$

Recalling that the dynamical map of the populations  $\mathcal{E}_p = \mathcal{P}_A \mathcal{U}_A \mathcal{P}_A$  can be expressed as in Eq. (24), we can state that

$$\begin{aligned} \mathcal{E}_p &= \mathcal{P}_A \mathcal{U}_A \mathcal{P}_A \\ &= \mathcal{E}_c^2 + \frac{1}{2} \mathcal{T}_{2,c} = \mathcal{P}_B \mathcal{U}_B \mathcal{P}_B \mathcal{U}_B \mathcal{P}_B + \frac{1}{2} \mathcal{P}_B \mathcal{U}_B \mathcal{Q}_B \mathcal{U}_B \mathcal{P}_B \\ &= \mathcal{P}_B \mathcal{U}_B \left( \mathcal{P}_B + \frac{1}{2} \mathcal{Q}_B \right) \mathcal{U}_B \mathcal{P}_B. \end{aligned} \quad (\text{E3})$$

Using this expression we can rewrite Eq. (E2) as

$$\begin{aligned} \mathcal{T}_{2,p} &= \mathcal{P}_A \mathcal{U}_A \mathcal{U}_A \mathcal{P}_A - \mathcal{P}_A \mathcal{U}_A \mathcal{P}_A \mathcal{U}_A \mathcal{P}_A = \\ &= \mathcal{P}_B \mathcal{U}_B (\mathcal{P}_B + \mathcal{Q}_B) \mathcal{U}_B \left( \mathcal{P}_B + \frac{1}{2} \mathcal{Q}_B \right) \mathcal{U}_B (\mathcal{P}_B + \mathcal{Q}_B) \mathcal{U}_B \mathcal{P}_B - \mathcal{P}_B \mathcal{U}_B \left( \mathcal{P}_B + \frac{1}{2} \mathcal{Q}_B \right) \mathcal{U}_B \mathcal{P}_B \mathcal{U}_B \left( \mathcal{P}_B + \frac{1}{2} \mathcal{Q}_B \right) \mathcal{U}_B \mathcal{P}_B \\ &= \frac{3}{2} (\mathcal{P}_B \mathcal{U}_B \mathcal{P}_B \mathcal{U}_B \mathcal{P}_B) (\mathcal{P}_B \mathcal{U}_B \mathcal{Q}_B \mathcal{U}_B \mathcal{P}_B) + \frac{3}{4} (\mathcal{P}_B \mathcal{U}_B \mathcal{Q}_B \mathcal{U}_B \mathcal{P}_B)^2 \\ &\quad + (\mathcal{P}_B \mathcal{U}_B \mathcal{Q}_B \mathcal{U}_B \mathcal{Q}_B \mathcal{U}_B \mathcal{P}_B) (\mathcal{P}_B \mathcal{U}_B \mathcal{P}_B) + \frac{1}{2} (\mathcal{P}_B \mathcal{U}_B \mathcal{Q}_B \mathcal{U}_B \mathcal{Q}_B \mathcal{U}_B \mathcal{Q}_B \mathcal{U}_B \mathcal{P}_B) \\ &= \frac{3}{2} \mathcal{E}_c^2 \mathcal{T}_{2,c} + \frac{3}{4} \mathcal{T}_{2,c}^2 + \mathcal{T}_{3,c} \mathcal{E}_c + \frac{1}{2} \mathcal{T}_{4,c} = \frac{3}{2} \mathcal{T}_{2,c} \mathcal{E}_p + \mathcal{T}_{3,c} \mathcal{E}_c + \frac{1}{2} \mathcal{T}_{4,c}. \end{aligned} \quad (\text{E4})$$

These derivations have used the fact that the components

of both the transfer tensors and the dynamical maps are scalars.